Towards Neutrino mass spectroscopy using atoms

M. Yoshimura @Okayama University
Experimental progress N. Sasao

- Why atoms for neutrino physics

- Unique way to distinguish Majorana from Dirac, and to determine the smallest neutrino mass

- Relic 1.9 K neutrino detection is feasible

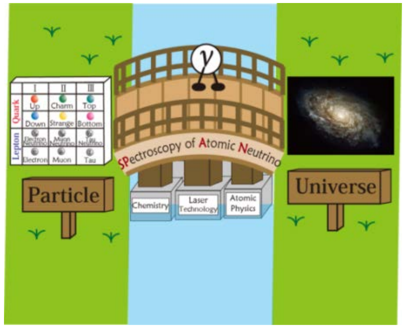

SPAN project

Search for the missing link of micro- and macro- worlds

Introduction

- What have been, and have not been, determined in neutrino experiments so far

- Remaining important questions on neutrino properties to probe physics beyond the standard theory and cosmology

Present status of neutrino physics

- Oscillation experiments
  - Finite mass
  - Flavor mixing
  - Only mass-squared difference can be measured.

$$U = VP\,, \tag{A8}$$

where

$$V = \begin{bmatrix} c_{12}c_{13} & s_{12}c_{13} & s_{13}e^{-i\delta} \\ -s_{12}c_{23} - c_{12}s_{23}s_{13}e^{i\delta} & c_{12}c_{23} - s_{12}s_{23}s_{13}e^{i\delta} & s_{23}c_{13} \\ s_{12}s_{23} - c_{12}c_{23}s_{13}e^{i\delta} & c_{12}c_{23} - s_{12}s_{23}s_{13}e^{i\delta} & c_{23}c_{13} \end{bmatrix}, \tag{A9}$$

with $c_{ij} = \cos\theta_{ij}$ and $s_{ij} = \sin\theta_{ij}$. The diagonal unitary matrix P may be expressed by

$$P = \mathrm{diag.}(1, e^{i\alpha}, e^{i\beta})\,, \tag{A10}$$

China, and Korea catched up

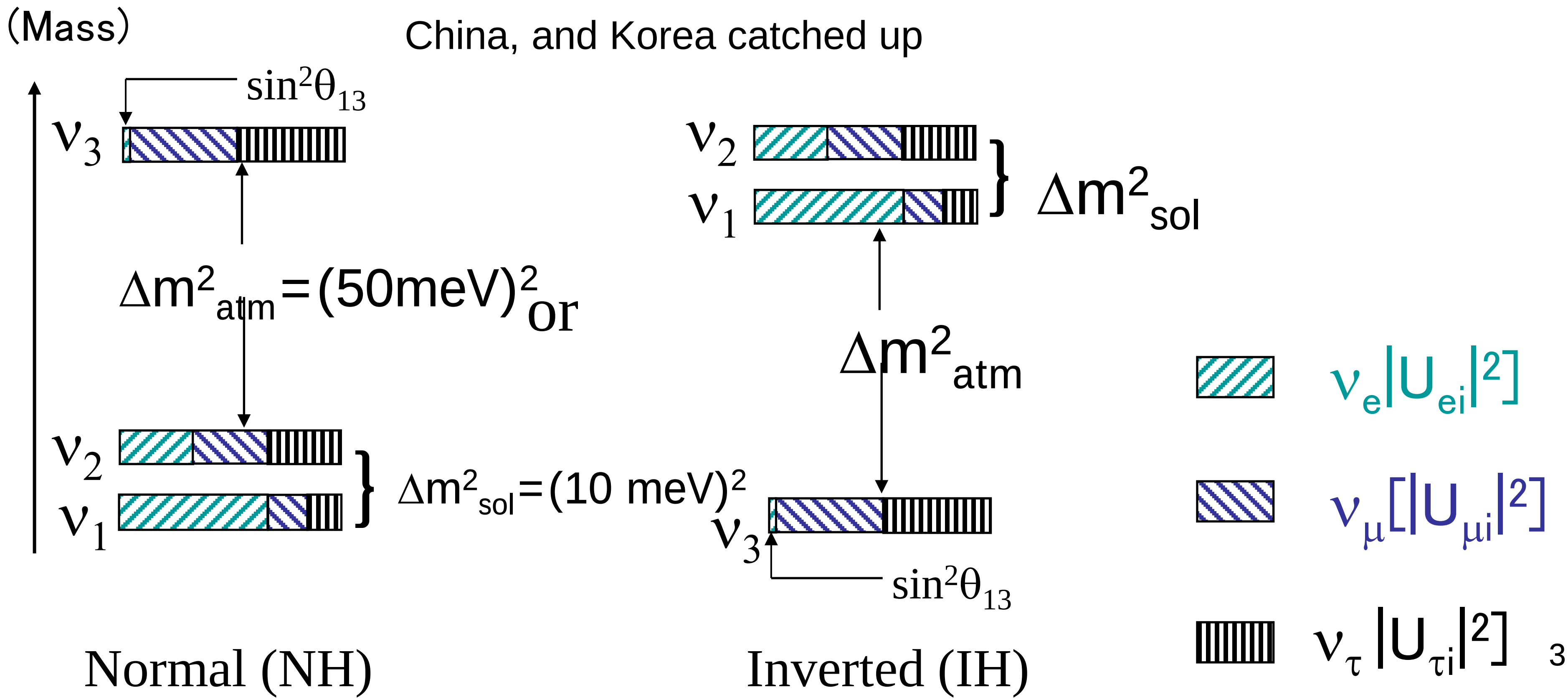

Important questions left in neutrino physics

- Absolute mass scale and the smallest mass (oscillation experiments are sensitive to mass squared differences alone)
- Majorana vs Dirac distinction
- CPV phase （Majorana case has 2 extra phases）

$$\alpha\,,\ \beta\,,\ \delta\ (\mathrm{KM-type})$$

These are relevant to explanation of matter-antimatter imbalance of universe.

We shall experimenttaly achieve all of these goals.

Our Okayama group has proposed an entirely new method using atoms, initiated R&D works and succeeded in establishing the huge rate enhancement in QED process, along with theoretical works.

Significance of Majorana neutrinos

- Plausible scenario of lepto-genesis

Heavy Majorana decay resposibe for generation of lepton asymmetry, being converted to baryon asymmetry via strong electroweak B, L violation keeping B-L conserved.

Prerequisite: ordinary neutrinos are also Majorana. New CPV sources related to heavy partners of mass >> Fermi scale

- Seesaw mechanism and an important step for construction of grand unified theory

$$\frac{m^2}{M}$$

Lepto-genesis

- Leading theory to explain the matter-antimatter imbalance of our universe
- Prerequisite: lepton number violation or Majorana type of mass, CP violation
- Sensitivity to low energy parameters Davidsson-Ibarra, NPB648, 345(2003)

CP asymmetry in leptogeneis

$$\approx \frac{3y_1^2}{4\pi}\left(-2(\frac{m_3}{m_2})^3 s_{13}^2 \sin 2(\delta+\alpha-\beta) + \frac{m_1}{m_2}\sin(2\alpha)\right)$$

+ (high energy phases inaccessible in low energy experiments)

$\text{Ours are sensitive to } \alpha\,,\ \beta-\delta\,;\ \ \text{the same as in lepto}-\text{genesis}$

Majorana vs Dirac equations: chirally projected solutions

Majorana eq. : particle=antiparticle

$$(i\partial_t - i\vec{\sigma}\cdot\vec{\nabla})\varphi = im\sigma_2\varphi^*$$

$$\varphi_{\vec{p},h}(x) = c(\vec{p},h)e^{-ip\cdot x}u(\vec{p},h) + c^\dagger(\vec{p},h)e^{ip\cdot x}\sqrt{\frac{E_p+hp}{E_p-hp}}(-i\sigma_2)u^*(\vec{p},h)\,,$$

$$u(\vec{p},h) = \frac{1}{2}\sqrt{\frac{E_p-hp}{pE_p(p+hp_3)}}\begin{pmatrix} p+hp_3 \\ h(p_1+ip_2)\end{pmatrix}\,.$$

2 neutrino wave functions are anti-symmetrized

Dirac eq.: degenerate 2 Majorana

$$(i\partial_t - i\vec{\sigma}\cdot\vec{\nabla})\varphi = m\chi\,,\quad (i\partial_t + i\vec{\sigma}\cdot\vec{\nabla})\chi = m\varphi$$

2-component in weak process involved

$$\psi_D = (1-\gamma_5)\psi/2$$

$$\psi_D = b(\vec{p},h)e^{-ip\cdot x}u(\vec{p},h) + d^\dagger(\vec{p},h)e^{ip\cdot x}\sqrt{\frac{E_p+hp}{E_p-hp}}(-i\sigma_2)u^*(\vec{p},h)$$

Particle annihilation Anti-particle creation

Majorana phase dependence

- Pair emission current at cross threholds

$$\langle (ip_1h_1\,, jp_2h_2)|j_\nu|0\rangle = \xi_i^*\xi_j e^{i(p_1+p_2)\cdot x} v_1^\dagger\sigma u_2 - \xi_i\xi_j^* e^{i(p_1+p_2)\cdot x} v_2^\dagger\sigma u_1$$
$$= e^{i(p_1+p_2)\cdot x}\left(i\Im\xi_i^*\xi_j(v_1^\dagger\sigma u_2 + v_2^\dagger\sigma u_1) + \Re\xi_i^*\xi_j(v_1^\dagger\sigma u_2 - v_2^\dagger\sigma u_1)\right)$$

$$\xi_i^*\xi_j = U_{ei}^*U_{ej} = c_{ij}^{(0)}\,, \quad U_{e1} = c_{12}c_{13}\,,\ U_{e2} = s_{12}c_{13}e^{i\alpha}\,,\ U_{e3} = s_{13}e^{i\beta}$$

Unless $(v_1^\dagger\sigma u_2 + v_2^\dagger\sigma u_1)$ and $(v_1^\dagger\sigma u_2 - v_2^\dagger\sigma u_1)$ are orthogonal, T-reversal violation $\propto \Im\xi_i^*\xi_j\Re\xi_i^*\xi_j$ can be measured, and all Majorana phases $\alpha\,,\beta$ are measurable. Non-orthogonality holds for $i \neq j$, or $m_i \neq m_j$.

$$\cos(2\alpha)\,, \quad \cos 2(\beta-\delta)\,, \quad \text{at } (12), (13), (23) \text{ thresholds}$$

Relevant atomic process to us

Radiative Emission of Neutrino Pair (RENP) from metastable atomic levels

- Process undoubtedly existing in standard theory, assuming finite neutrino masses

- Possible to amplify otherwise small rates by developing macro-coherence of a twin process

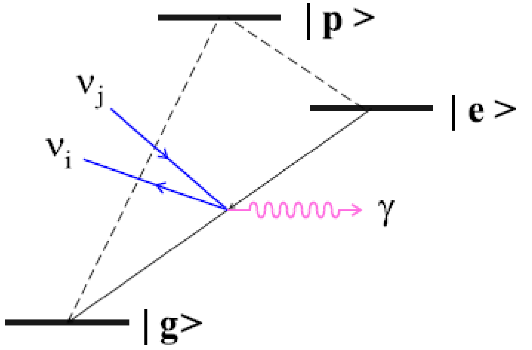

Neutrino weak interaction with electron and quarks in standard electroweak theory

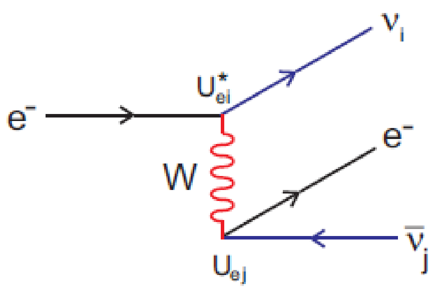

Charged Current

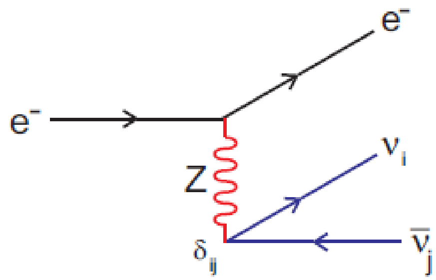

Neutral Current

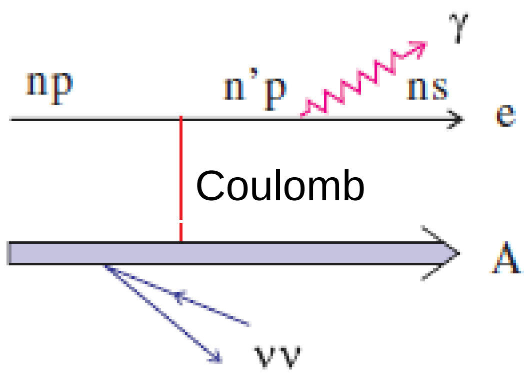

$$\mathcal{H}_{\rm eff} = \frac{G_F}{\sqrt{2}} \sum_{i,j} \bar{\nu}_i \gamma^\mu (1-\gamma_5)\nu_j \, \bar{e}\gamma_\mu (v_{ij} - a_{ij}\gamma_5) e ,$$

$$\mathcal{H}^q_{2\nu} \sim \frac{G_F}{\sqrt{2}} \sum_i \nu_i^\dagger (1-\gamma_5)\nu_i j^0_q ,$$

$$v_{ij} = U^*_{ei} U_{ej} - \left(\frac{1}{2} - 2\sin^2\theta_W \right) \delta_{ij} , \;\; a_{ij} = U^*_{ei} U_{ej} - \frac{1}{2}\delta_{ij} .$$

$$j^0_q = -\frac{1}{2} j^0_n + \frac{1}{2}(1 - 4\sin^2\theta_W) j^0_p ,$$

Mixing in W-exchange

$$U = VP , \tag{A8}$$

where

$$V = \begin{bmatrix} c_{12}c_{13} & s_{12}c_{13} & s_{13}e^{-i\delta} \\ -s_{12}c_{23} - c_{12}s_{23}s_{13}e^{i\delta} & c_{12}c_{23} - s_{12}s_{23}s_{13}e^{i\delta} & s_{23}c_{13} \\ s_{12}s_{23} - c_{12}c_{23}s_{13}e^{i\delta} & c_{12}c_{23} - s_{12}s_{23}s_{13}e^{i\delta} & c_{23}c_{13} \end{bmatrix} , \tag{A9}$$

with $c_{ij} = \cos\theta_{ij}$ and $s_{ij} = \sin\theta_{ij}$. The diagonal unitary matrix P may be expressed by

$$P = {\rm diag.}(1, e^{i\alpha}, e^{i\beta}) , \tag{A10}$$

Rate amplification by macroscopic coherence

- Super-radiance coherent volume (Dicke)
  - In case of SR, coherent volume is proportional to $\lambda^2 L$.
  - Phase decoherence time (T_2) must be longer than T_{SR}

$$\text{Rate} \propto \left| \sum_j^N e^{i\vec{k}\cdot\vec{r}_j} M_{atm} \right|^2 \propto N^2 \quad \left(\text{for } |r_j - r_l| \leq \lambda \right)$$

- For a process with plural outgoing particles
  - Phase matching condition (momentum conservation) is satisfied.
  - Coherent volume is not limited by λ., can be macroscopic.

$$\text{Rate} \propto \left| \sum_j^N e^{i(\vec{k}_1+\vec{k}_2+\vec{k}_3)\cdot\vec{r}_j} M_{atm} \right|^2 \propto N^2 \quad \left(\text{for } \vec{k}_1 + \vec{k}_2 + \vec{k}_3 = 0 \right)$$

Superradiance: 2 level and 1 photon case

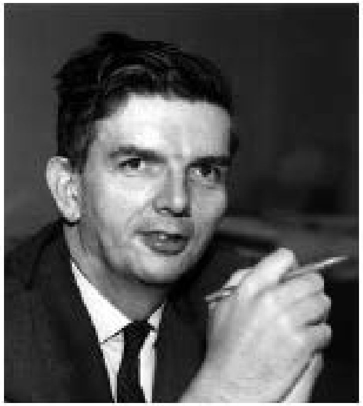

1916—1997

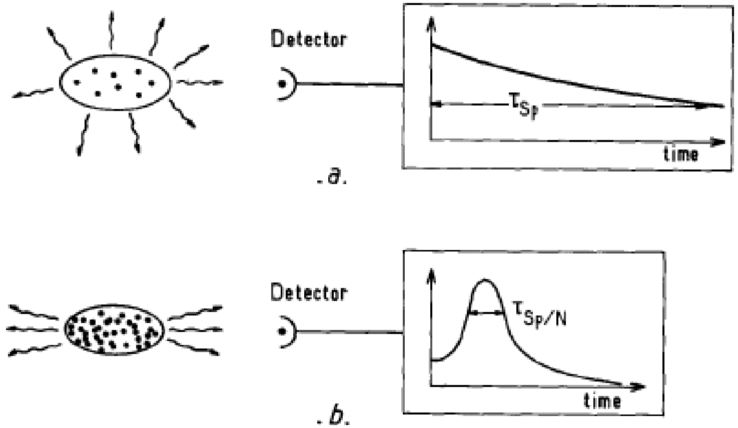

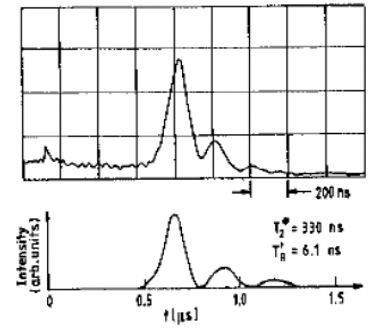

Figure 2.2. Oscilloscope trace of the super-radiance pulse observed by Skribanowitz *et al* [SHMF73] in HF gas at 84 μm ($J = 3 \rightarrow 2$), pumped by the $R_1(2)$ laser line, and the theoretical fit. The parameters are: pump intensity $I = 1$ kW cm^{-2}, $p = 1.3$ mTorr, $L = 100$ cm. The small peak on the oscilloscope trace at $t = 0$ is the 3 μm pump pulse, highly attenuated.

(PRL30(1973)309)

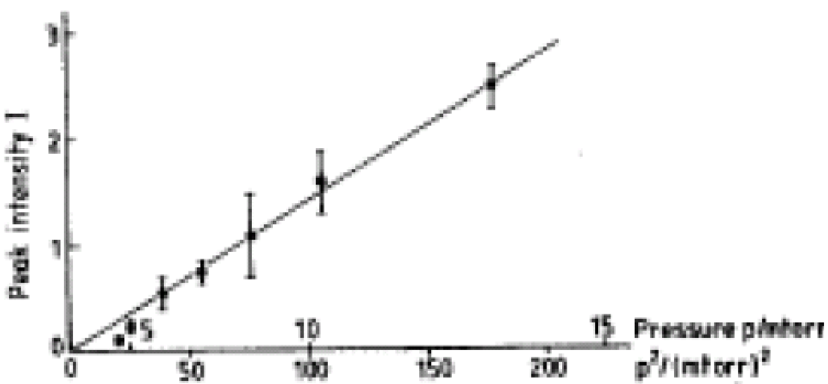

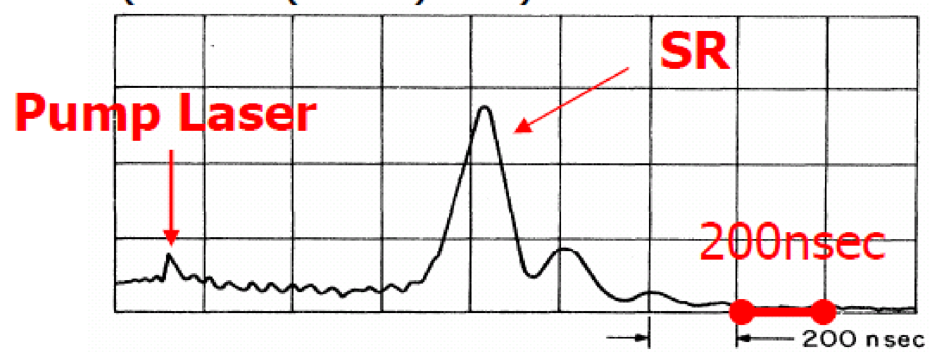

Rate enhanced by N

Delayed enhanced signal accompanied by ringing

m.yoshimura 09/2014

Radiative emission of neutrino pair (RENP)

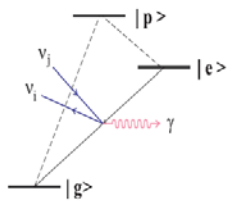

Fig. 1 Λ−type atomic level for RENP $|e\rangle \to |g\rangle + \gamma + \nu_i \nu_j$ with ν_i a neutrino mass eigenstate. Dipole forbidden transition $|e\rangle \to |g\rangle + \gamma + \gamma$ may also occur via weak M1× E1 couplings to virtual intermediate state $|p\rangle$.

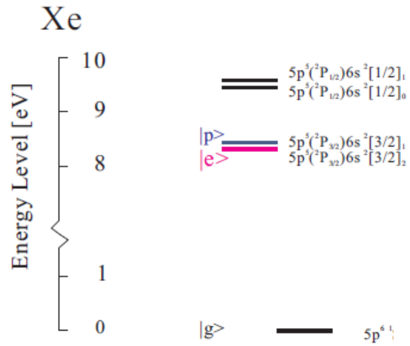

$$\Gamma = \Gamma_0 \; I(\omega) \; \eta(t)$$

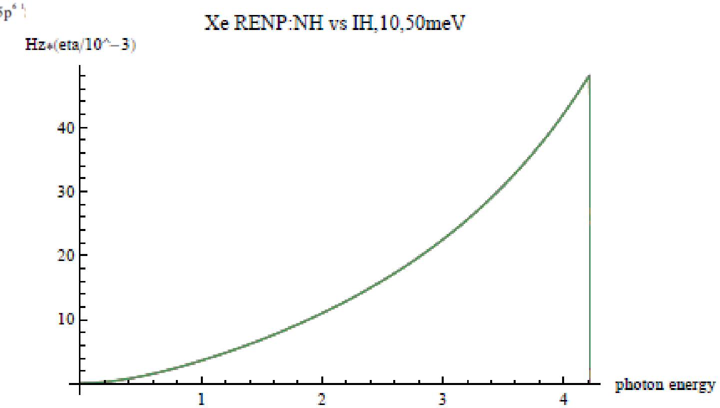

Six pair production thresholds
of mass eigen states

$$\omega_{ij} = \frac{\epsilon_{eg}}{2} - \frac{(m_i + m_j)^2}{2\epsilon_{eg}}$$

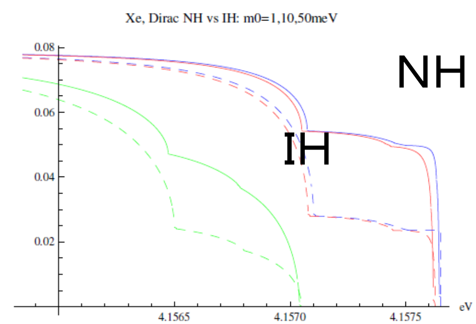

$$2^- \to 0^+$$

Due to energy and momentum conservation
Resolved by precision of trigger lasers

Fig. 2 RENP dimensionless spectrum function $I(\omega)$ near the neutrino pair emission thresholds from Xe level $5p^5(^2P_{3/2})6s^2[3/2]_2$. Neutrinos of the smallest mass of 1, 10 and 50 meV are taken for the normal (solid curve) and the inverted (dashed curve) hierarchical mass pattern.

Nuclear monopole rates

- Pair emission from nucleus (monopole) gives the largest rates

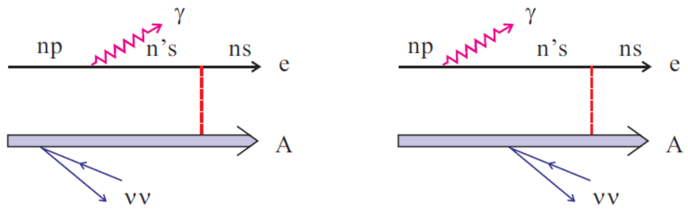

Figure 3: RENP diagrams 3 for alkali atoms.

$$Q_W^2 Z^{8/3}$$

$$Q_w \sim N - 0.044Z$$

Nuclear coherence effect

Spectrum rates for gas Xe

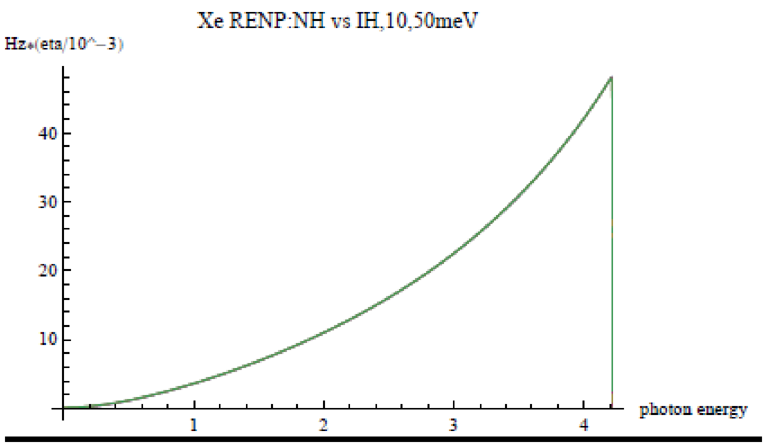

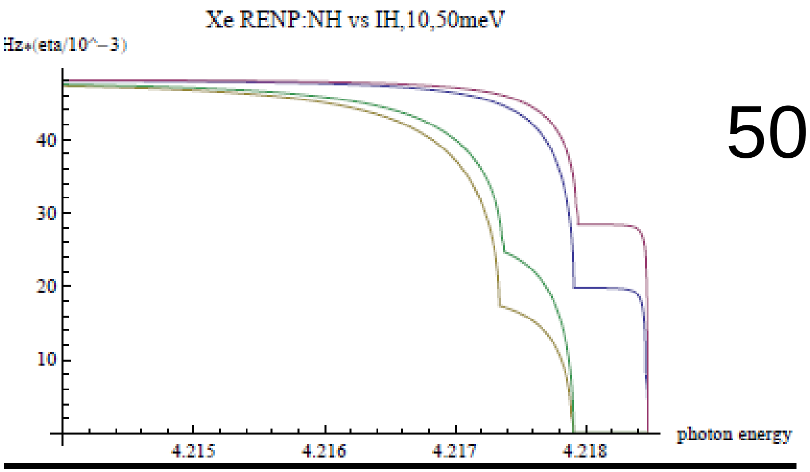

50 Hz

Dirac vs Majorana & CP phases

We need to go to the lower energy (smaller level spacing) to see CP phases.

Γ/Γ_0

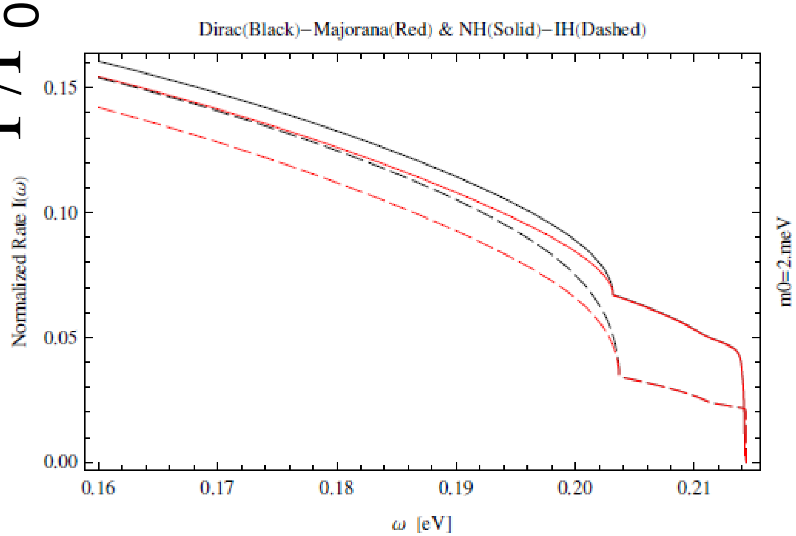

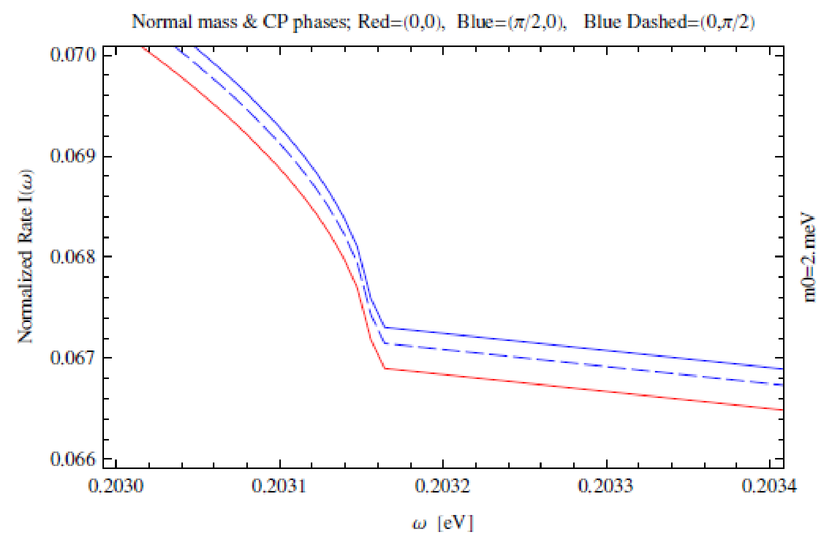

Eγ [eV]

Eeg= 0.429 eV
Epg= 0.446 eV

Eγ [eV]

Parity violating effects and asymmetric rates calculated: proof of involved weak interaction and important to increase S/N ratio

1. asymmetry under the magnetic field reversal,
2. asymmetry under the reversal of trigger photon circular polarization

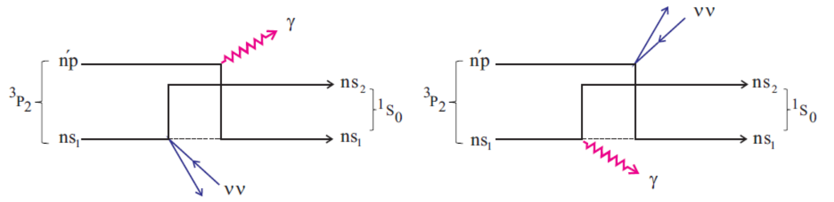

Figure 1: Parity odd contribution of valence electron exchange. Neutrino pair emission contains the PO part of vertex, as described in the text.

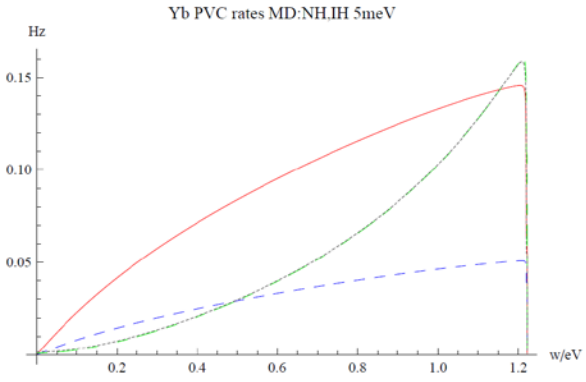

Figure 8: ${}^3P_2, J = 2, M_J = 1$ Yb PC rates, PV rate differences. Zeeman mixing amplitude 5×10^{-6} (corresponding to the magnetic field **), $\eta_\omega(t) = 1$, $n = 10^{22}\text{cm}^{-3}$, and 10^2cm^3 are assumed. Majorana NH PV in solid red, M-IH PV in dashed blue, M-NH PC rate divided by 50 in dash-dotted green, and M-IH/50 in dotted black (degenerate with M-NH PC).

PV rate much smaller than PC rate

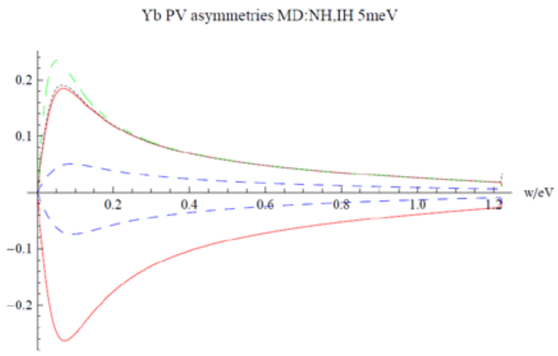

Figure 11: ${}^3P_2$Yb PV asymmetries vs photon energy. Zeeman mixing amplitude 5×10^{-6}, $\eta_\omega(t) = 1$, $n = 10^{22}\text{cm}^{-3}$, and a target volume 10^2cm^3 assumed. In the positive side the Majorana case of PV asymmetry under polarization reversal for NH is depicted in solid red, M-IH case in dashed blue, D-NH in dash-dotted green and the Dirac case for IH in dotted black. In the negative side PV asymmetry under the field reversal is plotted; M-NH and D-NH in solid red, and M-IH and D-IH in dashed blue, all assuming the smallest neutrino mass 5 meV.

MD distinction possible by measurement of PV asymmetry

Detection of relic neutrinos of 1.9 K

Recent work with N. Sasao and M. Tanaka

arXiv: 1409.3648

- Direct remnant at a few seconds after the big bang
- Prove that neutrinos were in thermal equilibrium, giving the important basis of light element synthesis such as 4He
- T differs from 2.7K of microwave, because electron-positron annihilation occurred after the neutrino decoupling at a few MeV, heating up matter in equilibrium
- Prediction is firm: (4/11)^(1/3) 2.7 K = 1.9 K, 110cm^-3

- Spectrum distortion by the Pauli blocking caused by ambient relic neutrinos

Neutrino distribution function

$$f(p) = \frac{1}{\zeta e^{\sqrt{p^2+m^2/(z_d+1)^2}/T}+1} \approx \frac{1}{\zeta e^{p/T}+1}$$

$$\zeta = e^{-\mu_d/T_d}\,, \qquad z_d = O(10^{10})$$

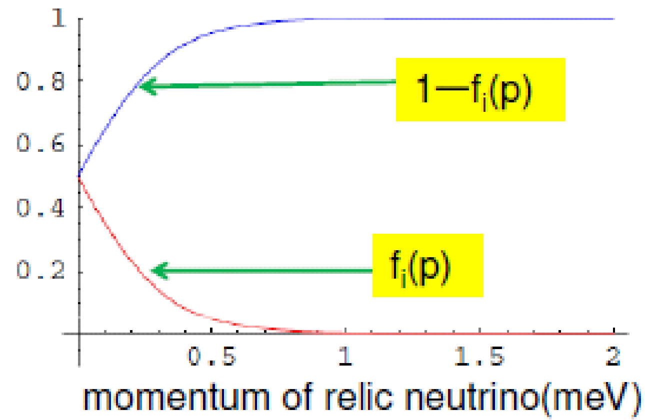

Blocking given by 1-f(p)

$$F_{ij}^A(\omega;T_\nu) = \frac{1}{8\pi\omega}\int_{E_-}^{E_+} dE_1\, g_{ij}^A(E_1)\cdot\left(1 - f(\sqrt{E_1^2 - m_i^2})\right)\left(1-\bar{f}(\sqrt{(\epsilon_{eg}-\omega-E_1)^2 - m_j^2})\right)\,,$$

$$g_{ii}^M(E) = -E^2 + (\epsilon_{eg}-\omega)E + \frac{1}{2}m_i^2 - \frac{1}{4}\epsilon_{eg}(\epsilon_{eg}-2\omega)+\delta_M\frac{m_i^2}{2}\,,$$

$$g_{ij}^S(E) = -\frac{1}{3}E^2+\frac{1}{3}(\epsilon_{eg}-\omega)E+\frac{1}{12}\epsilon_{eg}(\epsilon_{eg}-2\omega)-\frac{1}{12}(m_i^2+m_j^2)-\delta_M\frac{m_im_j}{2}\,,$$

$$E_\pm = \frac{1}{2}\left((\epsilon_{eg}-\omega)(1+\frac{m_i^2-m_j^2}{\epsilon_{eg}(\epsilon_{eg}-2\omega)})\pm\omega\Delta_{ij}(\omega)\right)\,, \quad \Delta_{ij}(\omega) = \left\{\left(1-\frac{(m_i+m_j)^2}{\epsilon_{eg}(\epsilon_{eg}-2\omega)}\right)\left(1-\frac{(m_i-m_j)^2}{\epsilon_{eg}(\epsilon_{eg}-2\omega)}\right)\right\}^{1/2}\,.$$

Temperature measurement possible for RENP ?

Ratio of rates: with to without Pauli blocking

with/without Pauli blocking

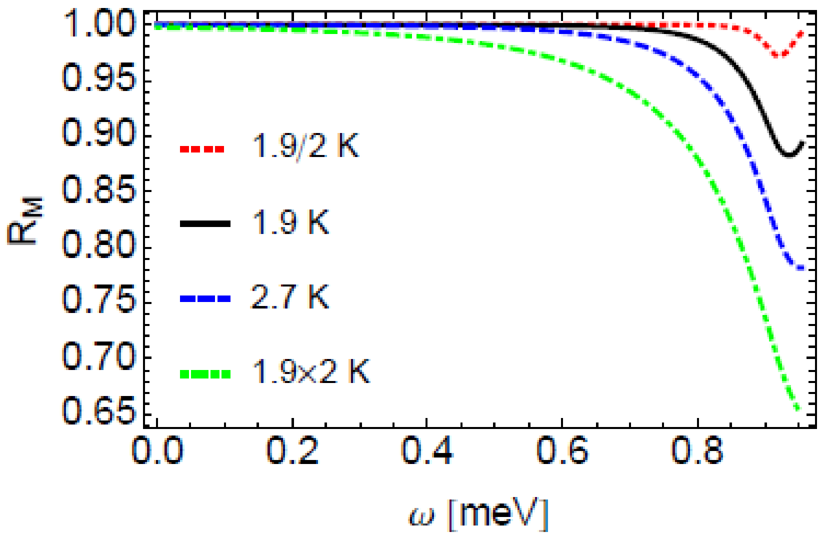

Difference of distortions for 1.9 and 2.7 K

10% level

For small level spacing, temperature measurement seems possible. Less sensitive than the inverse process.

Effect of chemical potential

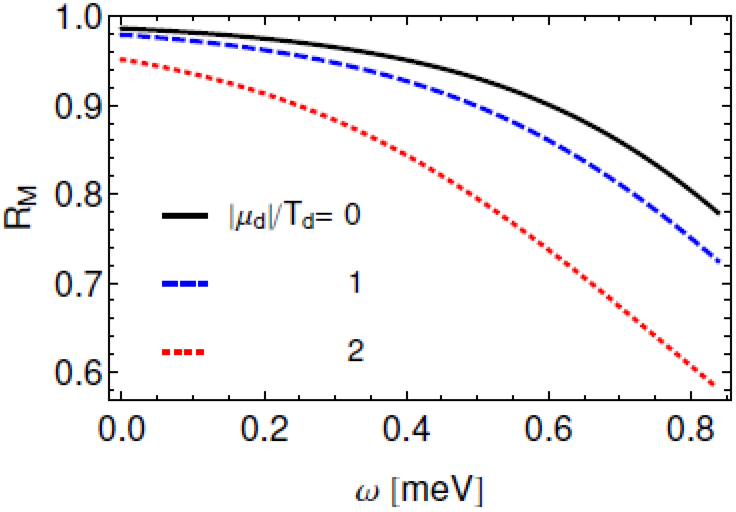

Figure 4: Spectrum distortion $R_M(\omega)$ for magnitudes of neutrino degeneracy $|\mu_d|/T_\nu = 0$ meV in solid black, 1 in dashed blue, and 2 in dotted red. The lightest neutrino mass $m_0 = 0$ meV. $\epsilon_{eg} = 10T_\nu \sim 1.7$ meV chosen.

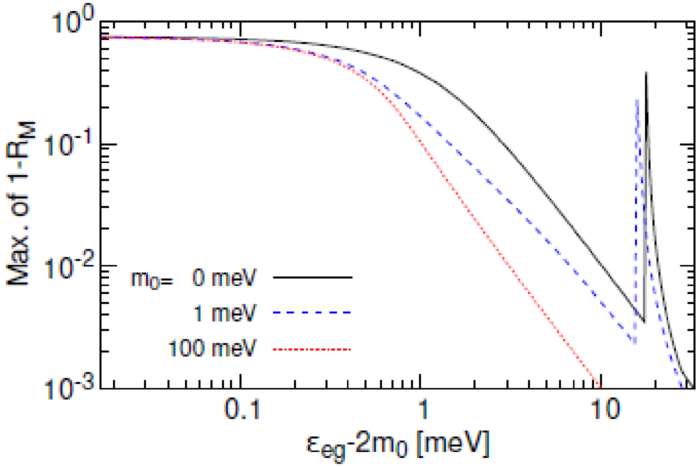

monopole

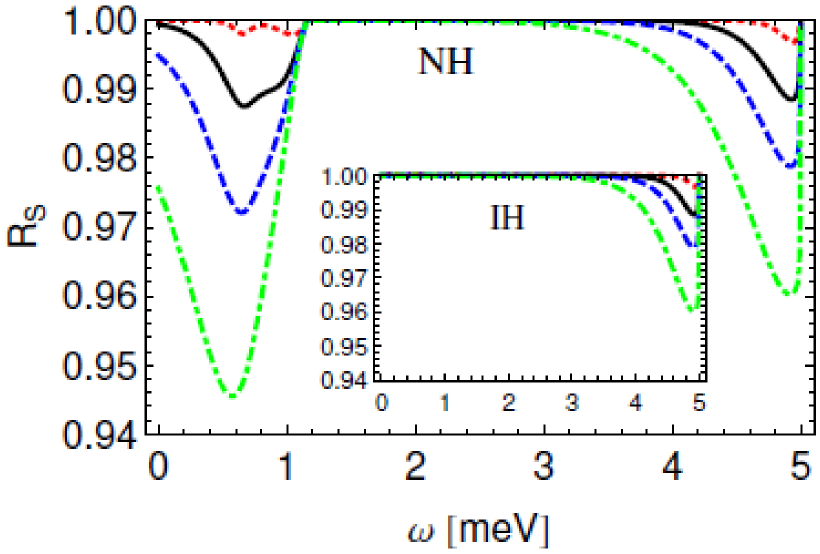

spin

Twin process: Paired Super-Radiance (PSR) important to develop large rates for RENP (also to prove the principle of macro-coherence)

- Macro-coherent amplification
  - A new type of coherent phenomena
  - Should be established experimentally
- Two photon emission process

$$|e\rangle \rightarrow |g\rangle + \gamma + \gamma$$

- Paired Super-Radiance
  - QED instead of weak process
  - Good experimental signature; i.e. back-to-back radiations with same color.

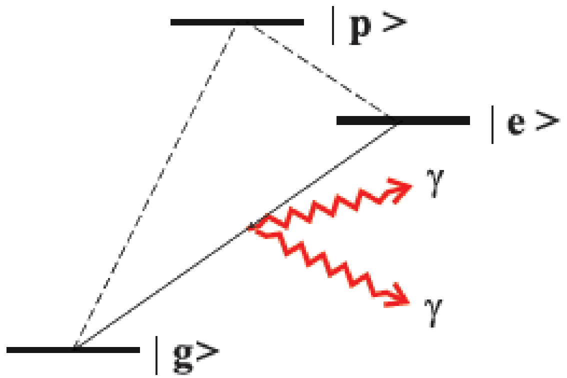

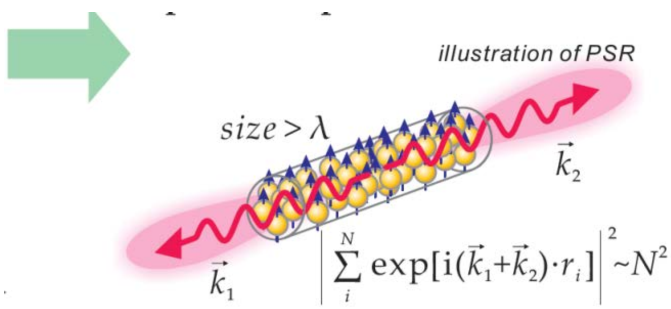

Effective 2-level model for trigger and medium evolution

2 level interaction with field

$$\frac{d}{dt}\begin{pmatrix} c_e \\ c_g \end{pmatrix} = -i\mathcal{H}\begin{pmatrix} c_e \\ c_g \end{pmatrix}, \quad -\mathcal{H} = 2\begin{pmatrix} \mu_{ee} & 2e^{i\epsilon_{eg}}\mu_{ge} \\ 2e^{-i\epsilon_{eg}}\mu_{ge} & \mu_{gg} \end{pmatrix} E^2$$

$$\text{Stark shifts}: \quad 2\times 2\,\text{Hamiltonian}$$

$$\text{Ba} \quad \begin{pmatrix} 6.0 & 2.1 \\ 2.1 & 16 \end{pmatrix} \text{GHz}\,\frac{|E|^2}{10^6\text{Wmm}^{-2}}$$

$$\text{Yb} \quad \begin{pmatrix} -1.2\times 10^{-7} & 1.7\times 10^{-4} \\ 1.7\times 10^{-4} & 6.6 \end{pmatrix} \text{GHz}\,\frac{|E|^2}{10^6\text{Wmm}^{-2}}$$

$$\text{Xe} \quad \begin{pmatrix} -8.4\times 10^{-11} & 1.5\times 10^{-5} \\ 1.5\times 10^{-5} & 0.22 \end{pmatrix} \text{GHz}\,\frac{|E|^2}{10^6\text{Wmm}^{-2}}$$

$$\text{Ca}^+ \quad \begin{pmatrix} 10 & 2.5 \\ 2.5 & 4.5 \end{pmatrix} \text{GHz}\,\frac{|E|^2}{10^6\text{Wmm}^{-2}}$$

$$\text{pH}_2 \quad \begin{pmatrix} 0.27 & 0.16 \\ 0.16 & 0.22 \end{pmatrix} \text{GHz}\,\frac{|E|^2}{10^6\text{Wmm}^{-2}}$$

$$\mu_{ee} = 2\sum_j \frac{d_{je}^2 E_{je}}{E_{je}^2 - \omega^2}, \quad \mu_{gg} = 2\sum_j \frac{d_{jg}^2 E_{jg}}{E_{jg}^2 - \omega^2}, \quad d_{ij} = \sqrt{3\pi\frac{\gamma_{ij}}{E_{ij}^3}}$$

$$\mu_{eg} = \sum_j \frac{d_{je}d_{jg}}{E_c - \delta\omega}, \quad \mu_{ge} = \sum_j \frac{d_{je}d_{jg}}{E_c + \delta\omega}.$$

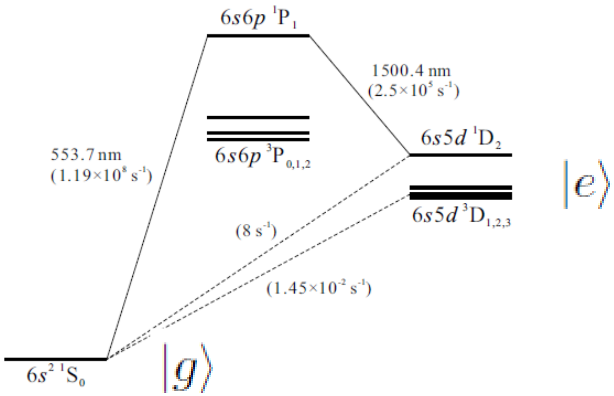

Ba

Maxwell-Bloch equation for PSR simulations: 1+1 dim

Bloch equation for medium

$$\vec{R} = \mathrm{tr}\ \rho\vec{\sigma} = \langle\psi|\vec{\sigma}|\psi\rangle$$

$$\partial_t R_1 = (\mu_{ee} - \mu_{gg})E^+E^-R_2 - i\mu_{ge}(e^{i\epsilon_{eg}}E^+E^+ - e^{-i\epsilon_{eg}}E^-E^-)R_3 - \frac{R_1}{T_2}\,,$$

$$\partial_t R_2 = -(\mu_{ee} - \mu_{gg})E^+E^-R_1 + \mu_{ge}(e^{i\epsilon_{eg}}E^+E^+ + e^{-i\epsilon_{eg}}E^-E^-)R_3 - \frac{R_2}{T_2}\,,$$

$$\partial_t R_3 = \mu_{ge}\left(i(e^{i\epsilon_{eg}}E^+E^+ - e^{-i\epsilon_{eg}}E^-E^-)R_1 - (e^{i\epsilon_{eg}}E^+E^+ + e^{-i\epsilon_{eg}}E^-E^-)R_2\right) - \frac{R_3 + n}{T_1}\,.$$

Field equation

$$(\partial_t^2 - \vec{\nabla}^2)\vec{E} = \vec{\nabla}^2\mathcal{D}\vec{E}\,,$$

$$-\mathcal{D}\vec{E}^+ = \left(\frac{\mu_{ee} + \mu_{gg}}{2}n + \frac{\mu_{ee} - \mu_{gg}}{2}R_3\right)\vec{E}^+ + \mu_{ge}e^{-i\epsilon_{eg}t}(R_1 - iR_2)\vec{E}^-\,.$$

SVEA (Slowly Varying Envelope Approximation)

$$E = \frac{1}{2}\left(e^{-i\omega_1(t-x)}E_R + e^{-i\omega_2(t+x)}E_L + (\mathrm{h.c.})\right)\,, \quad \omega_1 + \omega_2 = \epsilon_{eg}$$

complex amplitudes $E_R(x,t), E_L(x,t)$ slowly varying in 1+1 spacetime

- Coupled system of field and medium polarization highly non-linear

PSR simulations for two counter-propagating modes and soliton-condensates

Explosive PSR with initial coherence

para-H2 $n = 1 \times 10^{21}\,\mathrm{cm}^{-3}$, $L = 30\,\mathrm{cm}$, $T_1 = 1\,\mu s$, $T_2 = 10\,\mathrm{ns}$

Coherent initial state: $r_1 = 1,\ r_2 = r_3 = 0$

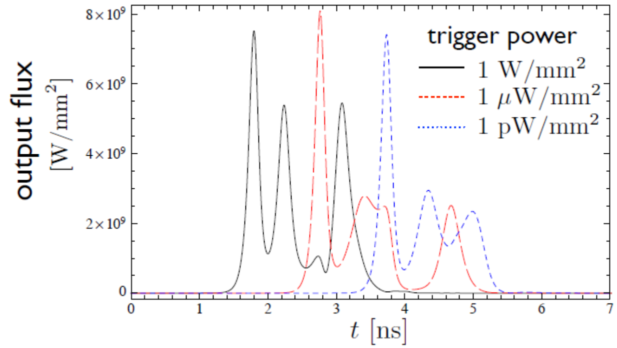

para-H_2 v=1->0

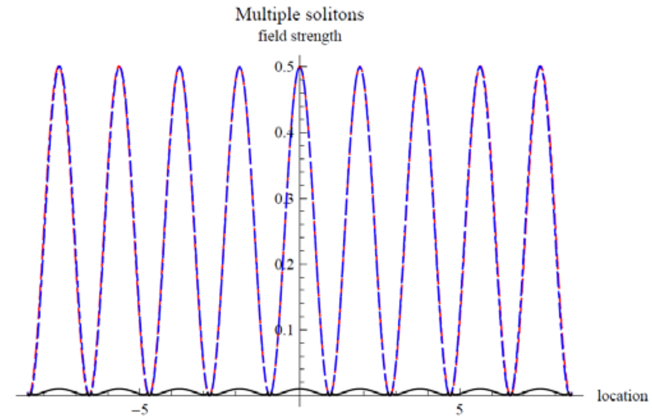

Minoru TANAKA

8

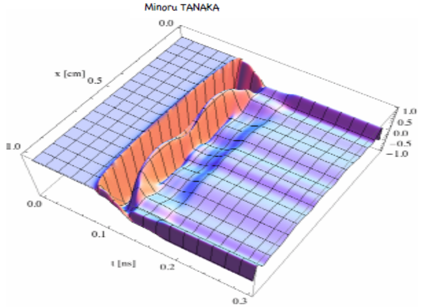

Figure 6: Spacetime profile of r_1 for the 1 Wmm^{-2} case of Fig(3).

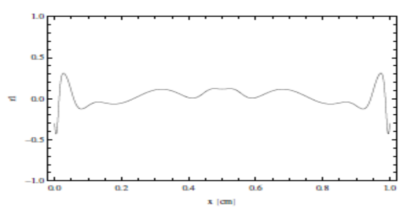

Figure 7: Spatial profile of r_1 at the latest time, 0.3 ns after trigger irradiation, of Fig(6).

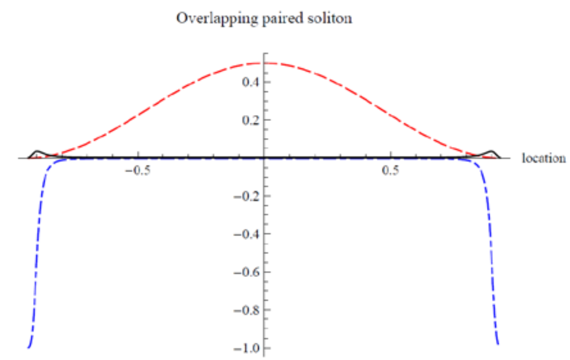

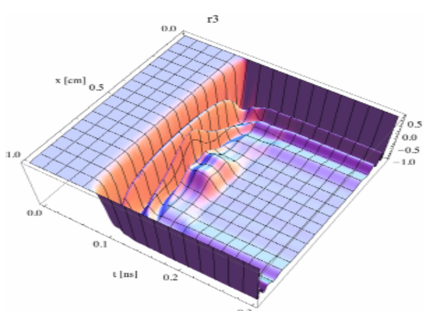

Figure 8: Spacetime profile of r_3 for the 1 Wmm^{-2} case of Fig(3).

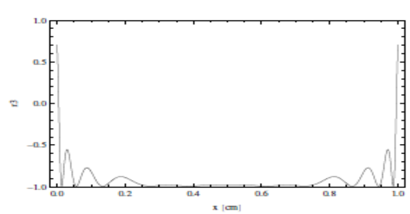

Figure 9: Spatial profile of r_3 at the latest time, 0.3 ns after trigger irradiation, of Fig(8).

Soliton-condensates stable against two-photon emission, unstable for RENP

m.yoshimura 09/2014

Experimental result (see Sasao)

- Linear growth region for two pair modes in the same direction
- Exponential time growth prop. to n * coherence, cut by de-coherence T_2

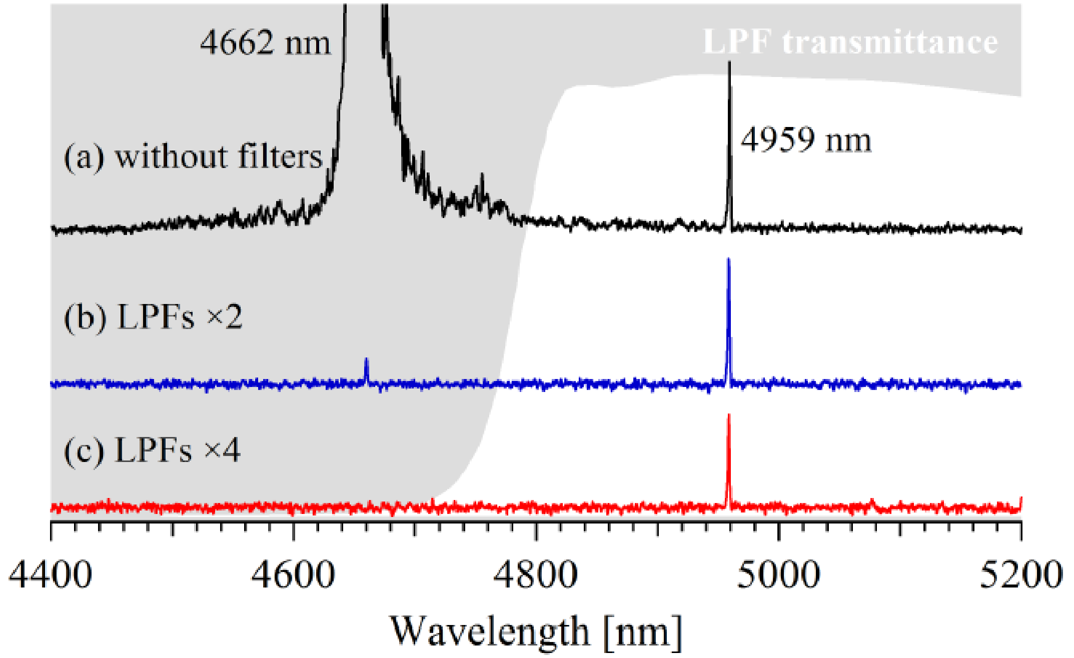

Twin process and controlled switching

RENP uses large medium polarization and stored fields by PSR, but two processes have different selection rules

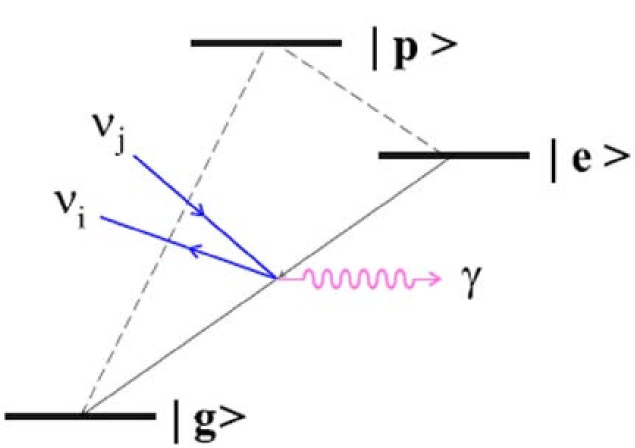

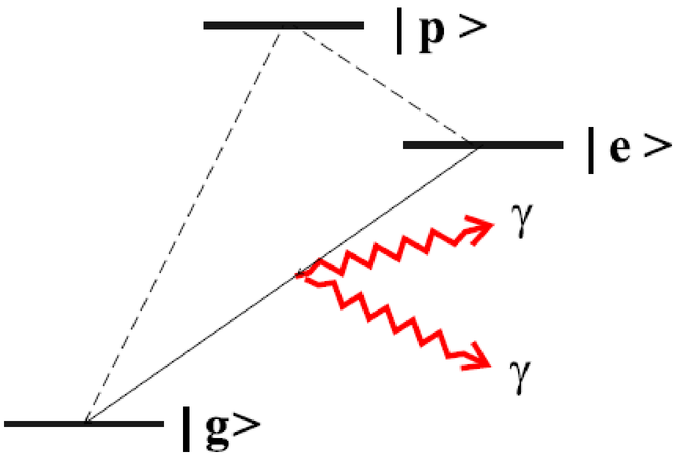

RENP: (E0 or M1)xE1 PSR: E1xE1

PSR-RENP switching is achieved by application of modulated E

Ideal state for RENP after PSR activity

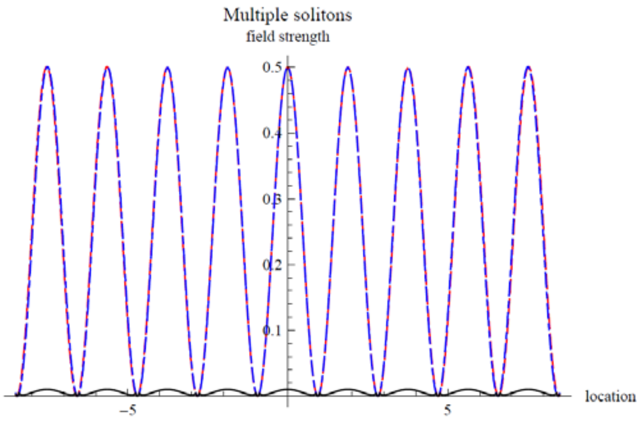

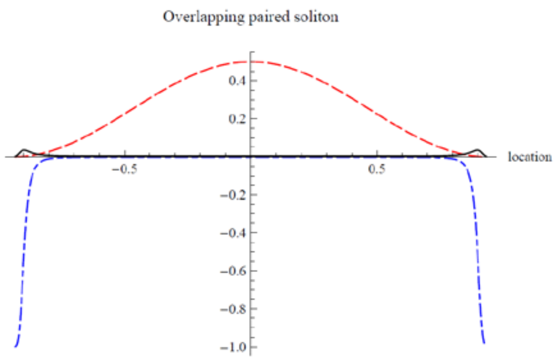

Soliton-condensates stable
against two-photon emission,
unstable for RENP

Analogue of
  stopped light
  polariton in cavity QED
Realized by two counter-propagating
 trigger PSR modes

Soliton-condensate formulated by non-linear eigenvalue problem

- Stationary solutions are derived from dynamical master eq. for PSR

$$\left(-E - \frac{d^2}{d\xi^2} - \mathcal{V}(e_i)\right)\begin{pmatrix} e_R \\ e_L^* \end{pmatrix} = 0\,,$$

Non-linear eigenvalue equation

$$\mathcal{V}(e_i) = \begin{pmatrix} \frac{\gamma_-}{2}(r_3(e_i)+1) & r_T^*(e_i) \\ r_T(e_i) & \frac{\gamma_-}{2}(r_3(e_i)+1) \end{pmatrix}$$

Forming potential well

$$r_1(e_i) = -\frac{4\tau_2}{D}\left(\Im(e_R e_L) + 2\tau_2\gamma_- \Re(e_R e_L)(|e_R|^2 + |e_L|^2)\right)\,,$$

$$r_2(e_i) = -\frac{4\tau_2}{D}\left(\Re(e_R e_L) - 2\tau_2\gamma_- \Im(e_R e_L)(|e_R|^2 + |e_L|^2)\right)\,,$$

$$r_3(e_i) = -\frac{1 + 4\gamma_-^2\tau_2^2(|e_R|^2 + |e_L|^2)^2}{D}\,, \qquad D = 1 + 4\gamma_-^2\tau_2^2(|e_R|^2 + |e_L|^2)^2 + 16\tau_1\tau_2|e_R e_L|^2\,,$$

Equivalent to particle motion in 2 dim.

$$\vec{r} = (e_R, e_L)$$

$$\vec{r}_\perp = (e_L, -e_R)$$

$$\frac{d^2\vec{r}}{d\xi^2} = \left(-E + \frac{r^2(r^2 - a^2\cos\theta_0)}{1 + r^4}\right)\vec{r} + \frac{a^2 r^2\cos\theta_0}{1 + r^4}\vec{r}_\perp\,,$$

$$a^2 = 8\frac{\tau_2}{\tau_1}\sqrt{\tau_2(\tau_1 + \gamma_-^2\tau_2)}\,, \qquad \tan\theta_0 = \frac{1}{4\gamma_-\tau_2}\,,$$

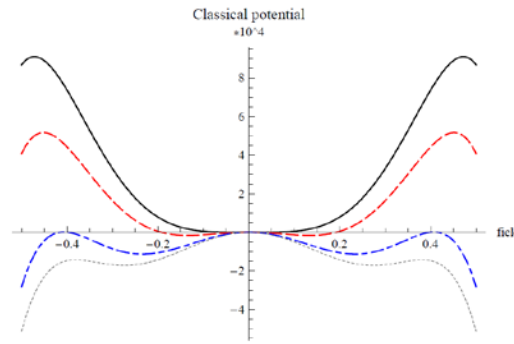

Experimental strategy towards neutrino mass spectroscopy

- 1st stage: proof of macro-coherence principle using QED (PSR)

- 2nd stage: control of PSR and soliton formation, switching between PSR and RENP modes, study of solid targets

- 3rd stage: discovery of the RENP process, measurements of mass matrix

Solid target: doped ions in ferro-electrics

- Large target number density required for PV measurements

- PSR <-> RENP mode switching effective

- Collaboration with specialists to be started

Summary

- Systematic neutrino mass spectroscopy is made possible when macro-coherence is realized and PSR is controlled by formation of soliton-condensate

- Not a joke, since the macro-coherent QED process (PSR) has been experimentally observed (next talk)